

Angular conductance resonances of quantum dots strongly coupled to noncollinearly oriented ferromagnetic leads

J. Fransson*

*Department of Materials Science and Engineering, Royal Institute of Technology (KTH), SE-100 44 Stockholm, Sweden
and Physics Department, Uppsala University, Box 530, SE-751 21 Uppsala, Sweden and NORDITA, Blegdamsvej 17, DK-2100
Copenhagen, Denmark*

(Received 11 February 2005; revised manuscript received 21 March 2005; published 8 July 2005)

The transport properties of quantum dots coupled to noncollinear magnetic leads is investigated. It is found that the conductance, and current, of the system in the strongly coupled regime is a nonmonotonic function of the angle between the magnetization directions in the two leads. Because of many-body interactions between electrons in the localized states of the quantum dot, induced by the presence of the conduction electrons in the leads, the positions of the quantum dot states are shifted in a spin-dependent way. Thus, the physics of the quantum dot is dynamically dependent on the angle between the magnetization directions of the two leads, which in combination with spin-flip transitions explains the nonmonotonic behavior of the magnetoresistance. The linear response conductance shows a rich complexity ranging from negative to positive magnetoresistance, depending on the positions of the localized states. The nonmonotonic transport characteristics persists for finite bias voltages.

DOI: [10.1103/PhysRevB.72.045415](https://doi.org/10.1103/PhysRevB.72.045415)

PACS number(s): 73.23.Hk, 73.63.Kv, 72.25.Mk, 85.75.-d

I. INTRODUCTION

Because of the fundamental complexities and far-reaching technological possibilities, the interest in spin-dependent transport in mesoscopic systems remain as high as ever. Since the first measurements of giant magnetoresistance (GMR) in Fe/Cr magnetic superlattices,¹ GMR effects on quantum dot (QD),²⁻⁶ and molecular^{5,7-10} systems have been reported. Moreover, magnetotransport has been studied for normal or ferromagnetic metallic islands,¹¹⁻¹⁶ and spin-dependent transport from ferromagnets through quantum dots.¹⁷⁻²² Recently, Kondo physics of QDs weakly coupled to ferromagnetic leads have been extensively studied,²³⁻²⁵ showing that a suppressed Kondo resonance due to the spin-polarization of the leads may be restored by application of an external magnetic field.

Thus far, the main focus has been devoted to systems with collinear magnetic alignment of the magnetic layers, or contacts.¹⁷⁻²² Recently, however, transport in systems with noncollinear magnetization orientations was addressed.²⁶⁻²⁹ Particularly, it was shown that the diodelike features in the transport characteristics of systems with one electrode being half-metallic are significantly reduced when the magnetic moments of the electrodes become noncollinear.²⁷

While one normally expects the maximal magnetoresistance in two-dimensional layered systems to be given by the resistance difference for antiparallel and parallel orientation of the magnetic layers, this is not necessarily true for a QD coupled to ferromagnetic leads. Because of the spatial smallness of the QD, its conductive states are zero-dimensionally confined, hence, the physical picture compared to multilayers is significantly different. The main reason is the, comparably, large on-site electron-electron (Coulomb) interaction present in QDs. Both theoretically and experimentally, it has been

shown that the Coulomb interaction is in the order of or larger than the level separation for QDs in the sizes of tens of nanometers.³⁰⁻³² The smallness of such systems allows one to generate a single-electron current through the system. Because of the large Coulomb repulsion, double-electron occupation of the QD will occur with a negligible probability. Then, since electrons in the strongly correlated QD states interact with the conduction electrons in the leads, the spin states in the QD are influenced by one another, which may lead to the two spin-channels becoming intermixed.

The mixing of the spin channels is an effect of kinematic (many-body) interactions between electrons in the localized QD states, which is induced by the presence of the conduction electrons in the contacts. By contacting the nonmagnetic QD by magnetic contacts, these interactions cause a spin-dependent shift of the localized state energies,¹⁹ which is comparable to the widths of the states and should therefore be measurable. The largest spin splitting of the localized states is caused by a parallel magnetic alignment of the contacts, whereas an antiparallel alignment gives the smallest spin split. For arbitrary noncollinear magnetic orientation of the contacts, the induced spin split becomes intermediate to the limiting cases, as expected. Finite on-site Coulomb interaction gives rise to lower and upper Hubbard states, and due to the renormalization caused by the kinematic interactions there appear four states in the QD. The energies and spectral weights of these states vary continuously with the magnetic orientation of the leads. This gives rise to a nonmonotonic dependence in the conductance, as well as in the magnetoresistance when the (equilibrium) chemical potential lies in the vicinity of either the lower or upper Hubbard states, that is, in the strongly coupled regime. In the weakly coupled regime, however, the system behaves with a normal spin valve. The different character of the transport properties in the two

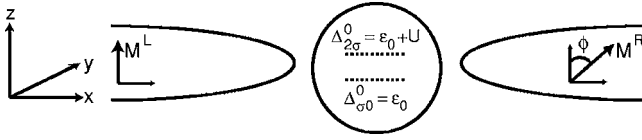


FIG. 1. The QD coupled to noncollinearly oriented ferromagnetic leads. The global reference frame and the magnetization M^L of the left reservoir coincide, while the magnetization M^R of the right reservoir is rotated by the angle ϕ . In the figure, the bare transition energies, $\Delta_{\sigma 0}^0 = \varepsilon_0$ and $\Delta_{2\sigma}^0 = \varepsilon_0 + U$ are indicated.

regimes can be explained by the variation of the current density at the chemical potential—a variation that is caused by the dynamical shift of the QD state energies and their corresponding spectral weights, and spin-flip transitions that occur with finite probability in noncollinear configurations. The nonmonotonic dependence in the conductance on the relative angle of the noncollinear magnetizations in the leads is predicted to be an effect of electron correlations, since the renormalization due to kinematic interactions vanishes at zero on-site Coulomb repulsion. Although the nonmonotonic characteristics of the transport properties are most striking in equilibrium, the behavior persists in nonequilibrium.

In this paper, the tunneling transport characteristics of a single-level QD attached to magnetic contacts in arbitrary noncollinear magnetic alignment is studied (see Fig. 1). The states in the QD are described in diagonal form, which enables the possibility to freely vary the electron-electron interaction parameter U . Thus tunneling through the QD via the two-particle state is also included. By means of an equation of motion combined with a diagrammatic technique³³ for the nonequilibrium many-body operator QD Green's function (GF), the many-body effects leading to the suggested results are included. The GF then is self-consistently calculated for each value of the chemical potential μ , bias voltage V , rotation angle ϕ , and temperature T , in order to account for fluctuations of the local QD properties under influence of the external variations. Choosing this method is motivated since it has previously³⁴ been shown to provide the essential nonequilibrium physics of single-level systems beyond the self-consistent Hartree-Fock, Hubbard I, approximation (HIA).^{35–38}

The paper is organized as follows. The QD system is defined and the equations for the transport calculations, and the local physical properties of the QD are briefly derived in Sec. II. The linear response conductance and nonequilibrium transport properties of the system is discussed in Sec. III, while the paper is summarized in Sec. IV.

II. MODELING THE SYSTEM

Consider a single level QD coupled to external contacts. Although the magnetization directions in the two contacts is noncollinear, it is useful to introduce a global spin reference frame, where the x direction lies along the direction of the charge current (see Fig. 1). As the global z direction is arbitrary around the x axis, there is no restriction in choosing it

along the local magnetization direction of the left reservoir, since its magnetic orientation is fixed, whereas the magnetization of the right reservoir is rotated by the angle ϕ in the global xz plane.

Suppose that the bare quantum dot level is spin degenerate at the energy ε_0 and that the on-site Coulomb repulsion is U , here the level spacing of the QD is assumed to exceed the thermal broadening. Hence, the energy of the QD is given by $\mathcal{H}_{QD} = \sum_{\sigma} \varepsilon_0 d_{\sigma}^{\dagger} d_{\sigma} + U n_{\uparrow} n_{\downarrow}$, where d_{σ}^{\dagger} (d_{σ}) creates (annihilates) an electron in the QD, whereas $n_{\sigma} = d_{\sigma}^{\dagger} d_{\sigma}$, and $\sigma = \uparrow, \downarrow$, is the spin projection in the global reference frame. In many cases, the Hubbard U is the largest parameter of the theory.^{30–32} However, in order not to make any restrictions on the correlation strength, the objective is to formulate a theory with a complete freedom in the strength of the Coulomb interaction, e.g., $0 \leq U < \infty$. Thus, the Hamiltonian \mathcal{H}_{QD} is transformed into diagonal form by introducing the Hubbard operators^{35,36} $X^{pq} = |p\rangle\langle q|$, which describe transitions from the $|q\rangle$ state and/or configuration to $|p\rangle$. The energy of the QD is, hence, given by $\mathcal{H}_{QD} = \sum_p E_p h^p$, where $h^p \equiv X^{pp}$, with the energies $\{E_0, E_{\sigma}, E_2\} = \{0, \varepsilon_0, 2\varepsilon_0 + U\}$ for the states $\{|0\rangle, |\sigma\rangle, |2\rangle \equiv |\uparrow\downarrow\rangle\}$.

The energies of the contact reservoirs are, for simplicity, given by $\mathcal{H}_{L/R} = \sum_{ks \in L/R} \varepsilon_{ks} c_{ks}^{\dagger} c_{ks}$, where c_{ks}^{\dagger} (c_{ks}), $k \in L/R$ creates (annihilates) an electron in the left or right (L/R) contact at the energy ε_{ks} with spin s . The ferromagnetism of the leads are modeled in the spirit of Stoner theory in the sense that a strong spin asymmetry in the density of states is assumed. The density of states is, moreover, approximated to be energy independent (while using structured density of states in real ferromagnets may modify details of the results, it will not change the general physical picture). The tunneling interaction between the left reservoir and the QD is given by (local reference frame coincides with the global)

$$\mathcal{H}_{TL} = \sum_{\substack{k\sigma \in L \\ a}} (v_{k\sigma} (d_{\sigma})^a c_{k\sigma}^{\dagger} X^a + \text{H.c.}), \quad (1)$$

where $v_{k\sigma}$ is the tunneling rate between the left lead and the QD, whereas $\sum_a (d_{\sigma})^a X^a = \langle 0 | d_{\sigma} | \sigma \rangle X^{0\sigma} + \langle \bar{\sigma} | d_{\sigma} | 2 \rangle X^{\bar{\sigma}2}$. Here, $\bar{\sigma}$ is the opposite spin of σ . The corresponding energy for the interaction between the QD and the right reservoir is given by, with the rotation of the magnetization direction included,

$$\begin{aligned} \mathcal{H}_{TR} = \sum_{k \in R} \{ & [(v_{k+} c_{k+}^{\dagger} \cos \phi/2 - v_{k-} c_{k-}^{\dagger} \sin \phi/2) (d_{\uparrow})^a \\ & + (v_{k+} c_{k+}^{\dagger} \sin \phi/2 + v_{k-} c_{k-}^{\dagger} \cos \phi/2) (d_{\downarrow})^a] X^a + \text{H.c.} \}, \end{aligned}$$

where $v_{k\pm}$ is the tunneling rate between the right lead and the QD. Here, the spin $s = \pm$ in order to distinguish between the global and local reference frames. The expression given in Eq. (3) can be conveniently rewritten by introducing the rotated QD operators

$$\begin{pmatrix} d_+ \\ d_- \end{pmatrix} = \begin{pmatrix} \cos \phi/2 & \sin \phi/2 \\ -\sin \phi/2 & \cos \phi/2 \end{pmatrix} \begin{pmatrix} d_r \\ d_l \end{pmatrix}. \quad (2)$$

Hence, Eq. (3) becomes

$$\mathcal{H}_{TR} = \sum_{\substack{ks \in R \\ a}} (v_{ks}(d_s)^a c_{ks}^\dagger X^a + \text{H.c.}). \quad (3)$$

A. Transport equations

The basic formula for the stationary current used in this paper is given by³⁹⁻⁴¹

$$\begin{aligned} J(\phi) = & -\frac{2e}{h} \text{tr} \text{Im} \int \{[\Gamma^L - \Gamma^R(\phi)]\mathbf{G}^<(\omega, \phi) \\ & + [f_L(\omega)\Gamma^L - f_R(\omega)\Gamma^R(\phi)][\mathbf{G}^r(\omega, \phi) - \mathbf{G}^a(\omega, \phi)]\} d\omega, \end{aligned} \quad (4)$$

where $\Gamma^{L/R}$ is the coupling between the left and right lead and the QD, whereas $\mathbf{G}^{<rla}$ is the lesser-retarded or advanced GF for the QD. The explicit ϕ dependence of the right coupling is appropriate since the spin dependence of the coupling varies as the magnetic orientation of the right lead is rotated. As will be shown in the Sec. II B, this angular dependence of the right coupling introduces an angle dependence of the QD GF. In Eq. (4), the Fermi function for the left or right lead at the chemical potential $\mu_{L/R}$ is denoted by $f_{L/R}(\omega) = f(\omega - \mu_{L/R})$.

In numerical calculations it is often convenient to rewrite the expression for the current in terms of only the lesser and larger GFs, e.g., $\mathbf{G}^{</>}$. This is possible because of the relation⁴² $\mathbf{G}^> - \mathbf{G}^< = \mathbf{G}^r - \mathbf{G}^a$. The current is then given in the form

$$\begin{aligned} J(\phi) = & -\frac{2e}{h} \text{tr} \text{Im} \int (\{f_L(\omega)\Gamma^L - f_R(\omega)\Gamma^R(\phi)\}\mathbf{G}^>(\omega, \phi) \\ & + \{[1 - f_L(\omega)]\Gamma^L - [1 - f_R(\omega)]\Gamma^R(\phi)\}\mathbf{G}^<(\omega, \phi)) d\omega. \end{aligned} \quad (5)$$

In equilibrium, this expression provides an account of the conductance of the system through the formula

$$\begin{aligned} G(\phi, \mu) \equiv & \left. \frac{\partial J}{\partial V} \right|_{V=0} \\ = & \frac{e^2}{h} \text{Re} \int \frac{\beta}{4} \cosh^{-2} \frac{\beta(\omega - \mu)}{2} \text{tr} \Gamma^L \mathbf{G}^r(\omega; \phi) \\ & \times \Gamma^R(\phi) \mathbf{G}^a(\omega; \phi) d\omega, \end{aligned} \quad (6)$$

where μ is the equilibrium chemical potential, $\Gamma^{L/R}$ is the tunneling rate between the left and right contact and the QD. For low temperatures, the function $\beta \cosh^{-2}(\beta[\omega - \mu]/2)/4 \rightarrow \delta(\omega - \mu)$, meaning that the expression in Eq. (6) qualitatively yields the equilibrium QD density of states, although

with altered amplitude, as the chemical potential is swept passed the positions of the transition energies.

B. Physics of the quantum dot

As was seen in the previous paragraph, Sec. II A, the conductance and/or current is given in terms of the local properties of the QD. These properties are obtained from the QD GF

$$G_{\sigma\sigma'}(t, t') = (-i) \frac{\langle \text{TS} d_\sigma(t) d_{\sigma'}^\dagger(t') \rangle}{\langle \text{TS} \rangle} = (d_\sigma)^a (d_{\sigma'}^\dagger)^{\bar{b}} G_{a\bar{b}}(t, t'), \quad (7)$$

(summation over double indices) where

$$G_{a\bar{b}}(t, t') = (-i) \frac{\langle \text{TS} X^a(t) X^{\bar{b}}(t') \rangle}{\langle \text{TS} \rangle}. \quad (8)$$

Here, a, b , denote Fermi-like (single-particle) transitions in the QD, whereas \bar{b} is the conjugate transition of b (e.g., if $X^b = X^{pq}$, then $X^{\bar{b}} = X^{qp}$). Note that the Hubbard operators describe changes in the configuration of the QD, here meaning that one electron that is either added or removed from the QD. In Eq. (8) the action $S = \exp[-i \int_{t_0}^{t_0 + \beta} \mathcal{H}'(t) dt]$, where the disturbance potential

$$\mathcal{H}'(t) = U_0(t) h^0 + \sum_{\sigma\sigma'} U_{\sigma\sigma'}(t) X^{\sigma\sigma'} + U_2(t) h^2 \quad (9)$$

contains the time-dependent source fields $U_\xi(t)$. These sources are used for the generation of a diagrammatic expansion of the QD GF in terms of functional derivatives with respect to the source fields. The integration is carried out along the contour in the complex plane, circumventing the positive real axis starting and ending at t_0 and $t_0 - i\beta$ ($\beta^{-1} = k_B T$), respectively.⁴² For convenience the notation $G_{a\bar{b}}(t, t') = (-i) \langle \text{TS} X^a(t) X^{\bar{b}}(t') \rangle_U$ is introduced in which the subscript U denotes the dependence of the GF on the disturbance source fields. Physical quantities are obtained from the GF in the limit $U_\xi(t) \rightarrow 0$, for the fields not actually applied to the system. The defined GF is well suited for studies of nonequilibrium phenomena and is easily converted into real-time GFs by means of the usual rules for analytical continuation (see for instance Refs. 34 and 43).

Following the procedure in Ref. 34, the equation of motion of GFs $G_{0\sigma\bar{a}}(i\omega)$, $G_{\bar{\sigma}2\bar{a}}(i\omega)$, are in the model

$$\mathcal{H} = \mathcal{H}_L + \mathcal{H}_R + \mathcal{H}_{QD} + \mathcal{H}_{TL} + \mathcal{H}_{TR} \quad (10)$$

given by

$$\begin{aligned} (i\omega - \Delta_{\sigma 0}^0 - \delta\Delta_{\sigma 0} - P_{0\sigma\bar{b}} V_{b\sigma 0}) G_{0\sigma\bar{a}}(i\omega) \\ = P_{0\sigma\bar{a}} + \eta_\sigma (P_{0\sigma\bar{b}} V_{b\sigma 0} + \delta\Delta_{2\bar{\sigma}}) G_{\bar{\sigma}2\bar{a}}(i\omega) \\ + \sum_{0\sigma\bar{\sigma}0} G_{0\sigma\bar{a}}(i\omega) + \sum_{\bar{\sigma}22\sigma} G_{\sigma 2\bar{a}}(i\omega), \end{aligned} \quad (11a)$$

$$\begin{aligned}
& (i\omega - \Delta_{2\bar{\sigma}}^0 - \delta\Delta_{2\bar{\sigma}} - P_{\bar{\sigma}2\bar{\sigma}}\bar{V}_{b2\bar{\sigma}})G_{\bar{\sigma}2\bar{a}}(i\omega) \\
& = P_{\bar{\sigma}2\bar{a}} + \eta_{\sigma}(P_{\bar{\sigma}2\bar{b}}\bar{V}_{b2\bar{\sigma}} + \eta_{\bar{\sigma}}\delta\Delta_{\sigma 0})G_{0\bar{\sigma}\bar{a}}(i\omega) \\
& + \sum_{0\bar{\sigma}\bar{\sigma}0}G_{0\bar{\sigma}\bar{a}}(i\omega) + \sum_{\bar{\sigma}22\sigma}G_{\sigma 2\bar{a}}(i\omega). \quad (11b)
\end{aligned}$$

Here $\Delta_{\bar{a}}^0$ is the bare energy for the transition a , whereas $\delta\Delta_{\bar{a}}$ is the renormalization energy due to kinematic interactions.^{19,34} The spectral weight of the GF (end factor) is denoted by $P_{ab}^-(t) = \langle T\{X^a, X^b\}(t) \rangle_U$. The interaction propagator $V_{ab}^- \equiv V_{ab}^-(i\omega) = \sum_{ks \in L,R} |v_{ks}|^2 (d_s^\dagger)^a (d_s)^b / (i\omega - \varepsilon_{ks})$, and the indices b denote summations over the transitions $\{0 \uparrow, 0 \downarrow, \downarrow 2, \uparrow 2\}$. The ‘‘backward’’ notation in V_{ab}^- is chosen since this provides a direct interpretation of Eq. (11) in terms of matrix multiplication. The prefactor $\eta_{\sigma} = \langle \bar{\sigma} | d_{\sigma} | 2 \rangle$ accounts for the selection rules among the involved transitions, where $\eta_{\uparrow, \downarrow} = 1, -1$, whereas $\langle 0 | d_{\sigma} | \sigma \rangle = 1$ for both $\sigma = \uparrow, \downarrow$.

As can be seen from Eq. (11), the general structure of the GFs G_{ab} can be written as $G_{ab} = D_{ac} P_{cb}$, where D_{ac} and P_{cb} are the locator and end factor, respectively.³³ The locator contains the local on-site properties of the GF, that is, the energetic position and width of the QD transition. The end factor, on the other hand, carries the spectral weight of the GF, which, in general, can be interpreted as sum of the population numbers of the involved states. The structure of Eq. (11) also provides the equation of motion directly as the 4×4 matrix equation

$$(i\omega I - \mathbf{\Delta}^0 - \mathbf{\Sigma})\mathbf{G}(i\omega) = \mathbf{P}, \quad (12)$$

where $\mathbf{\Delta}^0 = \text{diag}\{\Delta_{\uparrow 0}^0, \Delta_{\downarrow 0}^0, \Delta_{2\downarrow}^0, \Delta_{2\uparrow}^0\}$ (diagonal matrix) contains the bare transition energies, I is the identity matrix, whereas the self-energy matrix $\mathbf{\Sigma}(i\omega)$ can be written as $\mathbf{\Sigma}(i\omega) = \mathbf{P}\mathbf{V}(i\omega) + \delta\mathbf{\Delta}$. In this form, the interaction matrix is given by

$$\mathbf{V} = \mathbf{V}^L + \mathbf{V}^R = \mathbf{V}^L + \begin{pmatrix} \mathbf{v}^R & \sigma_z \mathbf{v}^R \\ \sigma_z \mathbf{v}^R & \mathbf{v}^R \end{pmatrix} \quad (13a)$$

$$\mathbf{V}^L = \sum_{k\sigma \in L} \frac{|v_{k\sigma}|^2}{i\omega - \varepsilon_{k\sigma}} \begin{pmatrix} \delta_{\sigma\uparrow} & 0 & \delta_{\sigma\uparrow} & 0 \\ 0 & \delta_{\sigma\downarrow} & 0 & -\delta_{\sigma\downarrow} \\ \delta_{\sigma\uparrow} & 0 & \delta_{\sigma\uparrow} & 0 \\ 0 & -\delta_{\sigma\downarrow} & 0 & \delta_{\sigma\downarrow} \end{pmatrix} \quad (13b)$$

$$\mathbf{v}^R = \sum_{ks \in R} \frac{|v_{ks}|^2}{i\omega - \varepsilon_{ks}} \mathcal{R}^T(\phi) \begin{pmatrix} \delta_{s+} & 0 \\ 0 & \delta_{s-} \end{pmatrix} \mathcal{R}(\phi), \quad (13c)$$

where

$$\mathcal{R}(\phi) = \begin{pmatrix} \cos \phi/2 & \sin \phi/2 \\ -\sin \phi/2 & \cos \phi/2 \end{pmatrix}, \quad (14)$$

and where σ_z is the z component of the Pauli spin vector. The coupling matrix $\mathbf{\Gamma}^{LR}$ is related to the retarded form of the interaction propagator, e.g., $\mathbf{\Gamma}^{LR} = -2 \text{Im}\mathbf{V}^{LR}(\omega + i\delta)$. In this paper the coupling $\mathbf{\Gamma}_{\sigma}^{LR}$ is parametrized in terms of $p_{LR} = (\mathbf{\Gamma}_{\uparrow}^{LR} - \mathbf{\Gamma}_{\downarrow}^{LR})/\Gamma_0$ by letting $\mathbf{\Gamma}_{\uparrow, \downarrow}^L = \Gamma_0(1 \pm p_L)/2$ and $\mathbf{\Gamma}_{\uparrow, \downarrow}^R = \Gamma_0(1 \pm p_R)/2$, where $\Gamma_0 = \mathbf{\Gamma}_{\uparrow}^{LR} + \mathbf{\Gamma}_{\downarrow}^{LR}$. Here, $\mathbf{\Gamma}_{\sigma}^{LR}$ defines the coupling between the spin channel σ in the left or right

lead and the QD. By this procedure no essential physics is lost, as discussed in Ref. 24. In terms of the spin-dependent parameters p_{α} the coupling matrices to the left and/or right lead become

$$\mathbf{\Gamma}^L = \frac{\Gamma_0}{2} \begin{pmatrix} 1+p_L & 0 & 1+p_L & 0 \\ 0 & 1-p_L & 0 & -1+p_L \\ 1+p_L & 0 & 1+p_L & 0 \\ 0 & -1+p_L & 0 & 1-p_L \end{pmatrix} \quad (15a)$$

$$\mathbf{\Gamma}^R = \begin{pmatrix} \gamma^R & \sigma_z \gamma^R \\ \sigma_z \gamma^R & \gamma^R \end{pmatrix} \quad (15b)$$

$$\gamma^R = \frac{\Gamma_0}{2} \begin{pmatrix} 1+p_R \cos \phi & p_R \sin \phi \\ p_R \sin \phi & 1-p_L \cos \phi \end{pmatrix} \quad (15c)$$

Finally, it is important to note that the end-factor matrix \mathbf{P} is block diagonal, e.g.,

$$\mathbf{P} = \begin{pmatrix} \mathbf{P}_1 & 0 \\ 0 & \mathbf{P}_2 \end{pmatrix},$$

where

$$\mathbf{P}_1 = \begin{pmatrix} N_0 + N_{\uparrow} & N_{\downarrow\uparrow} \\ N_{\downarrow\uparrow}^* & N_0 + N_{\downarrow} \end{pmatrix}$$

and

$$\mathbf{P}_2 = \begin{pmatrix} N_2 + N_{\downarrow} & N_{\downarrow\uparrow}^* \\ N_{\downarrow\uparrow} & N_2 + N_{\uparrow} \end{pmatrix},$$

explicitly interpreted as sums of the population numbers of the involved transitions. For a thorough survey of the method, the reader is referred to Refs. 33, 34, and 43.

From Eq. (12) it is clear that the equation of motion can be rewritten in the form of a Dyson-like equation, e.g.,

$$\mathbf{G} = \mathbf{g} + \mathbf{g}\mathbf{V}\mathbf{G}, \quad (16)$$

where $\mathbf{g} = (i\omega I - \mathbf{\Delta}^0)^{-1}\mathbf{P}$ is the QD GF in the atomic limit. Accordingly, one finds the retarded and/or advanced GF as

$$\mathbf{G}^{r/a} = \mathbf{g}^{r/a} + \mathbf{g}^{r/a}\mathbf{V}^{r/a}\mathbf{G}^{r/a}, \quad (17)$$

and the lesser and/or larger GFs as³⁴

$$\mathbf{G}^{</>} = \mathbf{G}'\mathbf{V}^{</>}\mathbf{G}^a. \quad (18)$$

Now, consider the renormalization energy $\delta\Delta_{\sigma 0} = \delta\Delta_{\sigma 0}^L + \delta\Delta_{\sigma 0}^R$ for the transition $X^{0\sigma}$, where

$$\delta\Delta_{\sigma 0}^L = \frac{1}{2\pi} \sum_{k \in L} |v_{k\bar{\sigma}}|^2 \int \frac{f(\varepsilon_{k\bar{\sigma}}) - f(\omega)}{\varepsilon_{k\bar{\sigma}} - \omega} \{-2 \operatorname{Im}[D_{0\bar{\sigma}\bar{\sigma}0}^r(\omega) + \eta_{\bar{\sigma}} D_{\sigma 2\bar{\sigma}0}^r(\omega)]\} d\omega \quad (19a)$$

$$\begin{aligned} \delta\Delta_{\sigma 0}^R = & \frac{\delta_{\sigma\uparrow}}{2\pi} \sum_{k \in R} \int \left\{ \left([f(\varepsilon_{k+}) - f(\omega)] \frac{|v_{k+}|^2}{\varepsilon_{k+} - \omega} \sin^2 \phi/2 + [f(\varepsilon_{k-}) - f(\omega)] \frac{|v_{k-}|^2}{\varepsilon_{k-} - \omega} \cos^2 \phi/2 \right) \{-2 \operatorname{Im}[D_{0\uparrow\downarrow 0}^r(\omega) + \eta_{\uparrow} D_{\uparrow 2\uparrow 0}^r(\omega)]\} \right. \\ & + \left. \frac{1}{2} \left([f(\varepsilon_{k+}) - f(\omega)] \frac{|v_{k+}|^2}{\varepsilon_{k+} - \omega} - [f(\varepsilon_{k-}) - f(\omega)] \frac{|v_{k-}|^2}{\varepsilon_{k-} - \omega} \right) \sin \phi \times \{-2 \operatorname{Im}[D_{0\uparrow\uparrow 0}^r(\omega) + \eta_{\uparrow} d_{\uparrow 2\uparrow 0}^r(\omega)]\} \right\} d\omega \\ & + \frac{\delta_{\sigma\downarrow}}{2\pi} \sum_{k \in R} \int \left\{ \left([f(\varepsilon_{k+}) - f(\omega)] \frac{|v_{k+}|^2}{\varepsilon_{k+} - \omega} \cos^2 \phi/2 + [f(\varepsilon_{k-}) - f(\omega)] \frac{|v_{k-}|^2}{\varepsilon_{k-} - \omega} \sin^2 \phi/2 \right) \times \{-2 \operatorname{Im}[D_{0\uparrow\uparrow 0}^r(\omega) + \eta_{\uparrow} D_{\uparrow 2\uparrow 0}^r(\omega)]\} \right. \\ & + \left. \frac{1}{2} \left([f(\varepsilon_{k+}) - f(\omega)] \frac{|v_{k+}|^2}{\varepsilon_{k+} - \omega} - [f(\varepsilon_{k-}) - f(\omega)] \frac{|v_{k-}|^2}{\varepsilon_{k-} - \omega} \right) \sin \phi \times \{-2 \operatorname{Im}[D_{0\uparrow\downarrow 0}^r(\omega) + \eta_{\downarrow} D_{\downarrow 2\uparrow 0}^r(\omega)]\} \right\} d\omega. \quad (19b) \end{aligned}$$

This expression gives a correction to the transition energy, e.g., $\Delta_{\sigma 0} = \Delta_{\sigma 0}^0 + \delta\Delta_{\sigma 0}$, arising because of kinematic interactions between particles in the different QD states induced by the presence of the reservoirs. The added contribution, the so-called loop correction,^{19,34,43} is a many-body effect that provides a bias voltage dependent shift of the transition energy. In addition, the shift strongly depends on the electronic and magnetic properties of the reservoirs. Thus, for instance magnetic contacts and/or spin-dependent tunneling probabilities induce a spin split in the QD, although the QD is nonmagnetic in the atomic limit.^{19,34,44} In the present case, this shift becomes strongly influenced by the noncollinearity of the magnetization directions of the contact reservoirs.

Analogous expressions can be derived for the other shifts. In fact, the renormalization term $\delta\Delta$ in the self-energy is a full 4×4 matrix, in general, and reduces to the case discussed in Ref. 34 only for collinear configured magnetic (and nonmagnetic) leads. In this sense the transition energies for the spin-flip transitions involved are also subject to renormalization due to the magnetism in the leads. However, the above expression [Eq. (19)] is displayed in order to illustrate some of the properties that are quite general to the loop correction. For instance, in both Eqs. (19a) and (19b) it is legible that the shift depends on the bias voltage through the presence of the Fermi functions. Thus, if a transition energy of the involved locators lies in the vicinity of the chemical potential of one (or both) reservoir(s), the shift will be larger than otherwise. The importance of this fact has previously been clearly demonstrated.^{19,43,45-47} It is also important to note that, although the energies for the transitions between the empty and singly occupied states are pushed downward from their corresponding bare energies due to the shift, the energies for the transitions between the singly and doubly occupied states are pushed upward.

More important in the present context, though, is that the shift strongly depends on the magnetic properties of the reservoirs. This is clear from Eq. (19), showing an explicit spin dependence of the couplings between the reservoirs and the QD. Hence, only when the couplings are equal are the induced shift of the QD transition energies exactly equal. In

contrast, the induced shifts are distinct whenever the couplings are unequal. This is illustrated in a simple example for the left part of the shift, $\delta\Delta_{\sigma 0}^L$. Assume that the magnetization directions in the two reservoirs are collinear, so that all off-diagonal locators vanish. For simplicity, also assume that $U \rightarrow \infty$, which leads to that propagators involving transitions between the one- and two-particle states can be neglected. Putting $D_{0\sigma\sigma 0}^r(\omega) = 1/(\omega - \Delta_{\sigma 0}^0 + i\delta)$, where $\Delta_{\uparrow 0}^0 = \Delta_{\downarrow 0}^0 (= \Delta_{10}^0)$ by construction, and where $\delta > 0$ is infinitesimal, reduces Eq. (19a) to

$$\delta\Delta_{\sigma 0}^0 = \frac{\Gamma_{\bar{\sigma}}^L}{2\pi} \log \left| \frac{\mu - \Delta_{10}^0}{\mu - W - \Delta_{10}^0} \right|,$$

where it has been assumed that the system is in equilibrium ($\mu_{L/R} = \mu$) and W is the width of the conduction band in the reservoir. For sufficiently large W , the ratio in the logarithm lies in the interval (0, 1), hence $\delta\Delta_{\sigma 0}^L < 0$. Assuming that W is large is not a severe restriction since $W \sim 1$ eV for normal metals used as contact reservoirs in real systems. Hence, the difference

$$\delta\Delta_{\uparrow 0}^L - \delta\Delta_{\downarrow 0}^L = \frac{1}{2\pi} \log \left| \frac{\mu - \Delta_{10}^0}{\mu - W - \Delta_{10}^0} \right| \left| \frac{\Gamma_{\downarrow}^L - \Gamma_{\uparrow}^L}{\Gamma_{\downarrow}^L} \right|$$

vanishes only if $\Gamma_{\uparrow}^L = \Gamma_{\downarrow}^L$. Note that the difference becomes negative (positive) if $\Gamma_{\uparrow}^L < \Gamma_{\downarrow}^L$ ($\Gamma_{\uparrow}^L > \Gamma_{\downarrow}^L$), meaning that $\Delta_{\uparrow 0} < \Delta_{\downarrow 0}$ ($\Delta_{\uparrow 0} > \Delta_{\downarrow 0}$). Consequently, contacting the QD by a magnetic reservoir to the left induces a spin split in the QD. The same argument can be used for the right contact and is certainly valid for finite U . The argument also holds for non-equilibrium situations, however, the equations become slightly more cumbersome to handle. It may also be noted that spin-dependent renormalization discussed here is consistent with the scaling result discussed in Ref. 23.

The spin-polarizing shifts of the transition energies induced from the left and right reservoirs provide a combined effect. This means that the induced spin split of the transition energies is maximal when the reservoirs are magnetically parallel, whereas the spin split is minimal for antiparallel

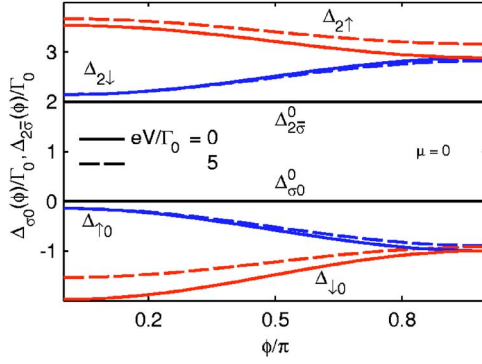


FIG. 2. (Color online). The angular dependence of the dressed transition energies in equilibrium (solid) and nonequilibrium (dashed) at the bias voltage $eV/\Gamma_0=5$. The bare transition energies $\Delta_{\sigma 0}^0$, $\Delta_{2\bar{\sigma}}^0$ are included for reference. Here, $\{\varepsilon_0, U, \mu\}/\Gamma_0=\{0, 2, 0\}$, and the spin asymmetry $p_{L/R}=0.85$ at $T/\Gamma_0=0.08$.

magnetic alignment (see Fig. 2). By a continuous rotation of the magnetization direction in the right reservoir ($0 \leq \phi \leq \pi$), the induced spin split will therefore continuously go from its maximum to its minimum, as can be seen in Fig. 2. Especially, in equilibrium (solid) the minimum spin split is zero when $\Gamma_{\sigma}^L = \Gamma_{\sigma}^R$, whereas in nonequilibrium (dashed) the finite bias voltage yields an unequal induced shift from the left and right reservoirs, which cause a difference between the state energies even in the antiparallel configuration, as can be seen in Fig. 2.

It should be pointed out that the renormalization because of kinematic interactions is a pure many-body effect, which is a characteristic feature of strongly correlated electron systems.^{19,38,45–47} Mathematically, it arises due to the non-trivial anticommutation relations between the Hubbard operators. Physically, however, the many-body effect is a result of the coupling between the correlated localized QD states because of the Coulomb repulsion and the hopping and mixing between the localized and delocalized states in the QD and the leads. This leads to the fact that the energy shift of the localized spin \uparrow state is influenced by the electron density in the other QD states which, in turn, are influenced by the presence of the delocalized electrons in the leads. Therefore, the energy of the spin \uparrow state becomes affected by the electronic and magnetic properties in the spin \downarrow channel.

Before leaving this section, it should be emphasized that correct values of the dressed transition energies are found only by solving the equations from self-consistent calculations. This is clear since the shift $\delta\Delta_{\bar{\alpha}}$ depends on the dressed locator $D_{b\bar{c}}^r$, hence the end-factors $P_{b\bar{c}}$, of all other transitions. In solving the system of GFs, the self-consistent loop contains several steps involving calculations of the transition energy shifts, defining the retarded and/or advanced and the lesser and/or larger QD GF, respectively, and calculating the population numbers $N_{\sigma} = \text{Im} \int [G_{0\sigma\sigma 0}^<(\omega) - G_{\sigma 22\sigma}^>(\omega)] d\omega$, $N_0 = -\sum_{\sigma} \text{Im} \int G_{0\sigma\sigma 0}^>(\omega) d\omega$, $N_2 = -\sum_{\sigma} \text{Im} \int G_{\sigma 22\sigma}^<(\omega) d\omega$, $N_{\sigma\bar{\sigma}} = -i \int [G_{0\bar{\sigma}\sigma 0}^< - G_{\sigma 22\bar{\sigma}}^>(\omega)] d\omega$, subject to the condition $1 = N_0 + \sum_{\sigma} N_{\sigma} + N_2$.⁴⁸ The self-consistent calculations have to be performed for all bias voltages, angles, positions of the transition energies, and couplings between the reservoirs and

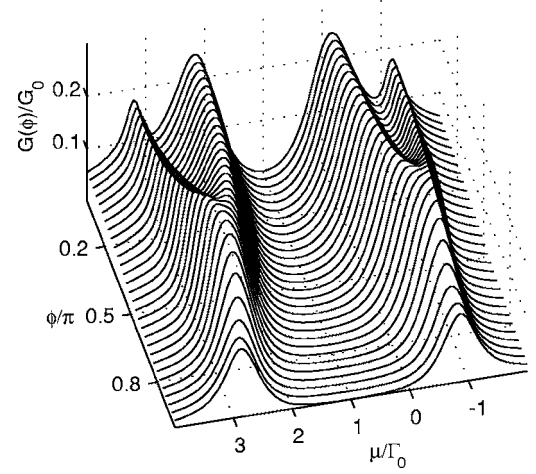


FIG. 3. Conductance $G(\phi)/G_0$ ($G_0=e^2/h$) as function of the rotation angle ϕ/π and equilibrium chemical potential μ/Γ_0 . Here, $\{\varepsilon_0, U, k_B T\}/\Gamma_0=\{0, 2, 0.08\}$ and the spin asymmetry $p_{L/R}=0.85$.

contacts. Consequently, the present results account for the physics of the system in a fashion that goes far beyond any master equation or conventional mean-field approach.

III. RESULTS

A. Equilibrium characteristics

A typical example of the equilibrium conductance $G(\phi)/G_0$ ($G_0=e^2/h$) is displayed in Fig. 3 as function of the rotation angle ϕ/π and the equilibrium chemical potential μ/Γ_0 . For $\phi/\pi=0$, that is parallel magnetic orientation of the reservoirs, it is readily seen that the system is resonant at four different energies due to the spin split of the QD level. As the angle increases, the difference between the transition energies $\Delta_{\uparrow 0}$ ($\Delta_{2\downarrow}$) and $\Delta_{\downarrow 0}$ ($\Delta_{2\uparrow}$) decreases, which confirms the behavior expected from Fig. 2. When studying the amplitude of the conductance G , it is striking that it is not a monotonic function of the angle whenever μ/Γ_0 is in the vicinity of any of the transition energies. From any linear response mean-field theory it is expected that the conductance varies with the local current density; here $j(\omega, \phi) \sim \text{tr} \text{Im} \Gamma^L \mathbf{G}^r(\omega; \phi) \Gamma^R(\phi) \mathbf{G}^a(\omega; \phi)$, at the chemical potential, and this picture is not altered here. However, the varying positions of the transition energies as functions of the angle provide an additional feature, namely, that the conductance is not necessarily maximal for parallel or antiparallel alignment of the magnetic reservoirs. It is also seen that the conductance is a strict monotonic function of ϕ/π whenever μ/Γ_0 lies either above or below the transition energies $\Delta_{\sigma 0}$ and $\Delta_{2\bar{\sigma}}$ or in the gap between them. Hence, the nonmonotonic characteristics of the conductance is predicted to be a feature of the strongly coupled regime, e.g., $|\Delta_{\sigma 0} - \mu|/\Gamma_0 \leq 1$ or $|\Delta_{2\bar{\sigma}} - \mu|/\Gamma_0 \leq 1$. In the weakly coupled regime (e.g., Coulomb blockade) the system returns to normal spin-valve characteristics.

In order to better understand the different regimes of the conductance one has to resort to study the current density at the chemical potential. In Figs. 4(a) and 4(b) the spin-

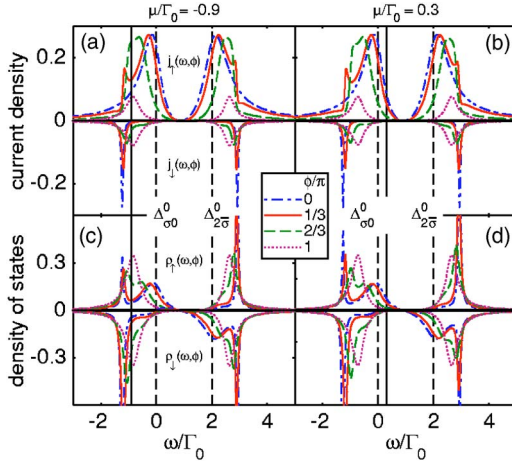


FIG. 4. (Color online). Spin-resolved $j_\sigma(\omega, \phi)$ (a, b) current density and (c, d) density of states $\rho_\sigma(\omega, \phi)$, for a few angles $\phi/\pi \in \{0, 1/3, 2/3, 1\}$ at (a) and (c), $\mu/\Gamma_0 = -0.9$, and (b) and (d), $\mu/\Gamma_0 = 0.3$. The positions of the chemical potential (solid), μ/Γ_0 , and the bare transition energy (dashed), $\Delta_{\sigma 0}^0/\Gamma_0 = 0$ and $\Delta_{2\bar{\sigma}}^0/\Gamma_0 = 2$, are shown for reference.

resolved current density at different chemical potentials and rotation angles is shown along with the corresponding spin-resolved density of states of the QD, Figs. 4(c) and 4(d). First, in the strong coupling regime [Figs. 4(a) and 4(c)], the chemical potential $\Delta_{\uparrow 0} < \mu < \Delta_{\downarrow 0}$ at $\phi/\pi = 0$ (dashed-dotted), whereas μ lies in the vicinity of $\Delta_{\uparrow 0} = \Delta_{\downarrow 0}$ at $\phi/\pi = 1$ (dotted). The current densities at the chemical potential in these limiting cases are related such that $j(\mu, 0) < j(\mu, \pi)$, which is expected since the total electron density at the chemical potential is higher in the antiparallel configuration [see Fig. 4(c)]. Thus, an increase in the rotation angle is expected to result in an increasing current density at μ/Γ_0 . However, the increasing current density at μ/Γ_0 eventually reaches a maximum for a specific rotation angle $0 < \phi^*/\pi < 1$, and a further increase of the rotation angle yields a decreased current density; hence, the maximum current density $j(\mu, \phi^*) > j(\mu, \pi) > j(\mu, 0)$. This character of the system is not expected from the density of states [Fig. 4(c)], which shows a monotonic increase of the density at μ/Γ_0 as ϕ/π is varied from 0 to 1. On the other hand, the density of states contains less information about the system's transport properties since $\rho(\omega, \phi) \sim -\text{tr Im } \mathbf{G}^r(\omega, \phi)$. Hence, although effects of spin-flip transitions are included into the QD GF, such make a larger impact on the current density than in the density of states. On a mathematical level this is understood because the current density is a matrix product of four nondiagonal matrices of which, at least, three contain information concerning spin-flip transitions in the system in the off-diagonal entries.

In the weakly coupled regime [Figs. 4(b) and 4(d)], the chemical potential lies between the transition energies $\Delta_{\sigma 0}$ and $\Delta_{2\bar{\sigma}}$, and the current density is readily seen to monotonically decrease as the rotation angle ϕ/π varies from 0 to 1. This is not surprising since the transition energies $\Delta_{\uparrow 0}$ and $\Delta_{\downarrow 1}$ lie closest to μ/Γ_0 when $\phi/\pi = 0$ and then moves away

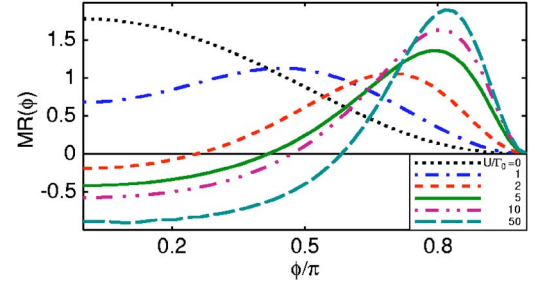


FIG. 5. (Color online). Magnetoresistance $MR(\phi)$ as function of the rotation angle for various values of the correlation strength U . Here, $\mu/\Gamma_0 = -0.9$ and other parameters as in Fig. 3

from the chemical potential as the $\phi/\pi \rightarrow 1$. Hence, both the density of states and current density at the chemical potential is monotonically reduced for increasing angles, resulting in a monotonically decreasing conductance.

Note in Figs. 4(c) and 4(d), that both spin projections of $\rho(\omega, \phi)$ acquires a finite density around the position of the opposite spin projection for $\phi/\pi < 1$. This is best seen in the spin \uparrow density. The reason for this is traced back to the fact that the channels are not independent (e.g., there is a finite probability for spin-flips to occur in the QD). Effects from such events are taken into account since the full nondiagonal matrix equation for the QD GF is solved in self-consistent calculations. Therefore, the densities for the two spin channels are peaked around both positions of the QD states. At $\phi = \pi$, however, the spin densities are only peaked around the position of its corresponding state, which does not mean that the channels are independent for this angle. Indeed, the spin split itself is a result of the strong correlations between the QD states.

In Fig. 5, the equilibrium magnetoresistance $MR(\phi) = [G(\phi) - G(\pi)]/G(\pi) \equiv [G(\phi) - G_{AP}]/G_{AP}$ as a function of the rotation angle is shown for various values of the correlation strength U , in the strong coupling regime. Here, the subscript AP refers to the antiparallel magnetic orientation of the leads; that is, $\phi/\pi = 1$. In the noncorrelated limit $U = 0$, the system behaves as a normal spin valve. As the QD states become correlated, the conductance varies nonmonotonically with the rotation angle, in agreement with the previous discussion. Increasing the strength of the correlations yields a remarkably high and relatively narrow peak in the conductance around the angle $\phi^*(\mu)$ ($\phi^*(\mu)/\pi \approx 0.8$ in the figure), depending on the chemical potential. As is known, the renormalization becomes increasingly important as the correlation between the states grows larger. This, in turn, leads to the fact that the spin split at ϕ/π grows larger with increasing U , implying a reduction of the electron density in the region between the state energies. Hence, it is expected that the conductance should decrease at ϕ/π as U grows, which is confirmed in Fig. 5. One can also note that $G(0) > G(\pi)$, positive magnetoresistance $MR(0) > 0$, for weak correlation, whereas for sufficiently strong correlations the relation is altered to $G(0) < G(\pi)$, negative magnetoresistance $MR(0) < 0$.

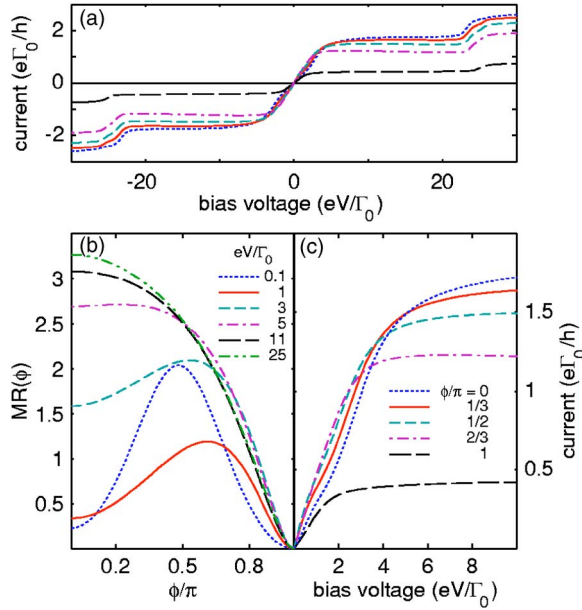


FIG. 6. (Color online). (a) J - V characteristics for various rotation angles, (b) angular dependence of the magnetoresistance for different bias voltages, and (c) detail of the J - V characteristics. Here, $\mu/\Gamma_0=0$, whereas $\{\varepsilon_0, U, k_B T\}/\Gamma_0=\{1.5, 10, 0.08\}$.

In the present paper all references to Kondo physics have been omitted since the main focus is devoted to nondegenerate configured systems. However, in the antiparallel regime for $\Gamma_\sigma^L=\Gamma_\sigma^R$, the system becomes degenerate in the sense that the spin split of the QD states vanishes. In this situation it would be expected to find a restored Kondo resonance at the chemical potential analogous to the results in Refs. 23–25. In the weakly coupled regime it would therefore be expected to find an enhancement of the conductance. This correlation effect would nonetheless not crucially affect the results in the strongly coupled regime, which is of main interest here, since any Kondo resonance would be smeared out by the main peak of the degenerate QD state in this regime.

B. Nonequilibrium characteristics

The nonmonotonic character of the conductance is closely related to the strong coupling regime, as discussed in Sec. III A. In nonequilibrium, this character is expected to be present for bias voltages such that $|\Delta_{\sigma 0}-\mu_{L/R}|/\Gamma_0 \ll 1$ or $|\Delta_{2\bar{\sigma}}-\mu_{L/R}|/\Gamma_0 \ll 1$, depending on which transition lies closest to the equilibrium chemical potential. It is that the current varies nonmonotonically with the rotation angle for bias voltages only around the “first” resonant transition, since the current gives an account of all available density within the window between the chemical potentials of the left and right leads. Thus, angular variations in the current density at higher voltages cause negligible deviations in the current compared to the total current. This is verified in Fig. 6, which shows (a) the current-voltage (J - V) characteristics for various rotation angles and (b) angular dependence of the nonequilibrium magnetoresistance $MR(\phi)=\{J(\phi)-J(\pi)\}/J(\pi) \equiv \{J(\phi)-J_{AP}\}/J_{AP}$ for different bias voltages, whereas (c)

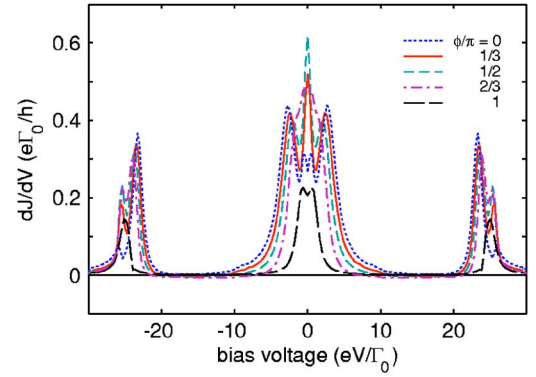


FIG. 7. (Color online). Differential conductance for various rotation angles, calculated as the numerical derivative of the J - V characteristics in Fig. 6(a).

displays the J - V characteristics at low bias voltages. In this case $|\Delta_{\sigma 0}^0-\mu|/\Gamma_0=1.5$, whereas $|\Delta_{2\bar{\sigma}}^0-\mu|/\Gamma_0=11.5$. In Fig. 6, it can be readily seen that the current varies nonmonotonically for low bias voltages, that is near resonance of $\Delta_{\sigma 0}$, whereas the system returns to a normal spin-valve character for larger biases. It should be noted in Fig. 6(a) that the plateau between the resonance of $\Delta_{\sigma 0}$ and $\Delta_{2\bar{\sigma}}$ is wider for large rotation angles than for lower. This is expected because of the larger spin separation of the transition energies at lower angles (c.f. Fig. 2). Especially, the distance between the highest transition between the empty and one-particle states ($|0\rangle\langle\sigma|$), and the lowest transition between the one- and two-particle states ($|\bar{\sigma}\rangle\langle 2|$) is minimal at $\phi/\pi=0$ and maximal at $\phi/\pi=1$ (see Fig. 2).

Now, although the current varies monotonically with the rotation angle at bias voltages such that the first resonant transition lies fully within the tunneling window, the differential conductance (dJ/dV) shows a nonmonotonic variation with the angle for voltages around the “second” resonance (see Fig. 7). However, this variation has little (or no) effect concerning the overall angular variation of the current, as previously discussed, which is also seen in Fig. 6.

It should be noted that the possibility of obtaining a non-monotonic angular dependence of the current is strictly related to that either $\Delta_{\sigma 0}-\mu < 0$ and $\Delta_{2\bar{\sigma}}-\mu < 0$, or $\Delta_{\sigma 0}-\mu > 0$ and $\Delta_{2\bar{\sigma}}-\mu > 0$. The reason is that the widths of the transition energies $P_{0\sigma}\Gamma_\sigma$ and $P_{2\bar{\sigma}}\Gamma_\sigma$ are strongly spin-asymmetric. For a majority spin σ in the leads (here giving $\Gamma_\sigma^{L/R} > \Gamma_{\bar{\sigma}}^{L/R}$), the transition energies are related according to $\Delta_{\bar{\sigma}0} < \Delta_{\sigma 0} < \Delta_{2\bar{\sigma}} < \Delta_{2\sigma}$. The width $P_{0\bar{\sigma}}\Gamma_{\bar{\sigma}}$ ($P_{2\sigma}\Gamma_{\bar{\sigma}}$) of the transition $|0\rangle\langle\bar{\sigma}|$ ($|\sigma\rangle\langle 2|$) is smaller than the width $P_{0\sigma}\Gamma_\sigma$ ($P_{2\bar{\sigma}}\Gamma_\sigma$) of the transition $|0\rangle\langle\sigma|$ ($|\bar{\sigma}\rangle\langle 2|$) (c.f. Fig. 4). Consequently, the angular dependent shift of the transition energy $\Delta_{\bar{\sigma}0}$ ($\Delta_{2\sigma}$) has a larger influence on the current density in the vicinity of the chemical potential than the corresponding shift of the transition energy $\Delta_{\sigma 0}$ ($\Delta_{2\bar{\sigma}}$). When all transition energies lie on either side of the equilibrium chemical potential, the first resonant transition is relatively narrow ($|0\rangle\langle\bar{\sigma}|$ or $|\sigma\rangle\langle 2|$), whereas the second and third are wider as the bias voltage grows. Then, around the rather

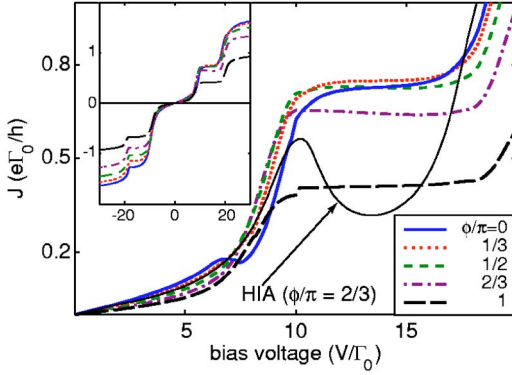


FIG. 8. (Color online). Current for various rotation angles. The current resulting from the HIA at $\phi/\pi=2/3$ is shown as reference. Inset showing the current over a wider bias voltage interval. Here $\{\varepsilon_0, U, k_B T\}/\Gamma_0 = \{5, 4, 0.08\}$ and $p_L = 0.4$ and $p_R = 1$.

sharp first resonance, there may be a possibility to recognize the angular variation of the transition energy in a nonmonotonic angular variation of the current. On the other hand, if the transition energies $\Delta_{\sigma 0}$ and $\Delta_{2\bar{\sigma}}$ lie on each side of the equilibrium chemical potential, then the first resonant transition ($|0\rangle\langle\sigma|$ or $|\bar{\sigma}\rangle\langle 2|$) is sufficiently wide to smear out any possible nonmonotonic angular variation of the current.

Finally, the difference between the present and earlier results is addressed. In a previous paper,³⁴ the technique used in the present paper was shown to provide the essential nonequilibrium physics of a single-level system beyond the self-consistent Hartree-Fock, or Hubbard I, approximation (HIA).^{35–38} For instance, it was shown that the introduced loop correction, which gives a renormalization of the localized state energies due to correlation effects, removes instances of unphysical negative differential conductance (NDC) that occurs in the HIA. This qualitative difference was found both in nonmagnetic as well as in magnetic systems, which thus motivates the present study. Recent studies on similar systems was performed by means of density-matrix approach,²⁸ which did not include the noncorrelated case ($U=0$), and with nonequilibrium GFs in the HIA.²⁹ Both of these approaches are unable to include the here-discussed on-site correlations effects. In particular, the latter study may yield conclusions of NDC, for certain configurations, as an artifact of the approximation. By also including effects of on-site correlations into the formalism, the occurrence of such NDC in the region between the one- and two-particle transitions found in Ref. 29 cannot be supported. In the present formulation, the HIA is obtained by omitting the renormalization $\delta\Delta$.^{19,34} Therefore, the QD transition energies remain bare, hence spin-degenerate, in the HIA although the couplings to the left and/or right lead are spin-dependent. Accordingly, there will be a larger energy gap between the transition energies $\Delta_{\uparrow 0}^0 = \Delta_{\downarrow 0}^0$ and $\Delta_{2\downarrow}^0 = \Delta_{2\uparrow}^0$ than with inclusion of the loop correction. As the bias voltage varies in this gap, the spin dependence of the leads (in terms of the couplings $\Gamma_{\sigma}^{L/R} > \Gamma_{\bar{\sigma}}^{L/R}$) provides a higher occupation of the transition $|0\rangle\langle\sigma|$ ($|\bar{\sigma}\rangle\langle 2|$) than for the other. This, in turn, leads to

a decreasing current in the gap. The current then increases as the “second” transition becomes resonant (see Ref. 34). An example of the resulting current can be viewed in Fig. 8 (faint) at $\phi/\pi=2/3$.

When the loop correction is included, however, the gap between the transitions $|0\rangle\langle\sigma|$ and $|\bar{\sigma}\rangle\langle 2|$ is smaller, see previous discussion. In addition, the electron density is redistributed such that the higher (lower) of the transition energies $\Delta_{\uparrow 0}$ ($\Delta_{2\downarrow}$) and $\Delta_{\downarrow 0}$ ($\Delta_{2\uparrow}$) acquires a significantly larger width than the lower (higher). The redistribution of the spectral weights then tends to prevent a sufficiently high occupation in any of the transitions required for a blockade of the transport. The plots in Fig. 8 display the current calculated with the loop correction for various rotation angles, clearly showing the absence of any significant NDC for all angles. Only in the case $\phi/\pi=0$ is there a clear NDC, which is related to the comparably large spin split of the transition energies $\Delta_{\downarrow 0}$ and $\Delta_{\uparrow 0}$ in the parallel configuration and the significantly smaller width of the lower transition, which permits a sufficiently high occupation of that transition in order to effectively block the current in a small range of the bias voltage. A deeper analysis of this particular case is, however, beyond the scope of the present paper.

IV. CONCLUSIONS

It has been demonstrated that the transport characteristics (equilibrium conductance and nonequilibrium current) of single-level QDs with arbitrary correlation U , coupled to ferromagnetic leads in noncollinear magnetic orientation in the strongly coupled regime display a clear nonmonotonic variation of the angle between the magnetic directions in the leads. The behavior is related to electron correlations between the states and the presence of spin-flip transitions in the system for finite angles ($0 < \phi/\pi < 1$) between the magnetic orientations of the leads. The correlation effects tend to induce an angular dependence of the transition energies, generating a decreasing spin split of the transition energies as the magnetic orientation of the leads is varied from the parallel to antiparallel configuration. Because of the spin-flip transitions, the amplitude of the current density at the chemical potential varies nonmonotonically with the rotation angle that provides the nonmonotonic transport characteristics, although the density of electron states at the chemical potential displays a monotonic variation.

The nonmonotonic transport characteristics are absent in the noncorrelated case ($U=0$), while its presence for $U>0$ leads to the conclusion that the effect is intimately associated with electron correlations of the localized states. In addition, the correlation effects included in the description tend to remove occurrence of NDC, found in the HIA,²⁹ for bias voltages in the gap between the “first” and “second” resonance. Since the transition energies spin split due to the spin-dependent properties of the leads (and/or the coupling between the leads and the QD), the spectral weight of the different transitions redistribute, which leads to a reduction of the gap between the first and second resonance.

Experiments on single-level QDs coupled to magnetic

contacts where the magnetization of the contacts can be rotated relative to each other would be very intriguing and would provide valuable information to the general understanding of magnetoresistive effects in nanostructured systems, as well as the significance of electron correlations in nanostructured materials.

ACKNOWLEDGMENTS

The author thanks O. Eriksson and O. Bengone for helpful discussions. Support from the Carl Trygger Foundation, the Göran Gustafsson's Foundation, and the Swedish Foundation for Strategic Research (SSF) is acknowledged.

*Electronic address: Jonas.Fransson@fysik.uu.se

- ¹M. N. Baibich, J. M. Broto, A. Fert, F. Nguyen Van Dau, F. Petroff, P. Etienne, G. Creuzet, A. Friederich, and J. Chazelas, *Phys. Rev. Lett.* **61**, 2472 (1988).
- ²J. P. Bird, K. Ishibashi, Y. Aoyagi, and T. Sugano, *Superlattices Microstruct.* **16**, 161 (1994).
- ³M. Stopa, J. P. Bird, K. Ishibashi, Y. Aoyagi, and T. Sugano, *Phys. Rev. Lett.* **76**, 2145 (1996).
- ⁴D.-J. Kim, J.-J. Kim, K. W. Park and H. C. Kwon, *Phys. Rev. B* **65**, 075314 (2002).
- ⁵B. R. Bulka and S. Lipiński, *Phys. Rev. B* **67**, 024404 (2003).
- ⁶R. López and D. Sánchez, *Phys. Rev. Lett.* **90**, 116602 (2003).
- ⁷M. Zwolak and M. Di Ventra, *Appl. Phys. Lett.* **81**, 925 (2002).
- ⁸H. Zare-Kolsaraki and H. Micklitz, *Phys. Rev. B* **67**, 094433 (2003).
- ⁹R. Pati, L. Senapati, P. M. Ajayan, and S. K. Nayak, *Phys. Rev. B* **68**, 100407(R) (2003).
- ¹⁰W. I. Babiacyk and B. R. Bulka, *J. Phys.: Condens. Matter* **16**, 4001 (2004).
- ¹¹K. Ono, H. Shimada, and Y. Ootuka, *J. Phys. Soc. Jpn.* **66**, 1261 (1997).
- ¹²J. Barnas and A. Fert, *Phys. Rev. Lett.* **80**, 1058 (1998).
- ¹³S. Takahashi and S. Maekawa, *Phys. Rev. Lett.* **80**, 1758 (1998).
- ¹⁴A. Brataas, Y. V. Nazarov, J. Inoue, and G. E. W. Bauer, *Phys. Rev. B* **59**, 93 (1999).
- ¹⁵J. Barnas, J. Martinek, G. Michalek, B. R. Bulka, and A. Fert, *Phys. Rev. B* **62**, 12363 (2000).
- ¹⁶J. Martinek, J. Barnas, S. Maekawa, H. Schoeller, and G. Schön, *Phys. Rev. B* **66**, 014402 (2002).
- ¹⁷W. Rudziński and J. Barnas, *Phys. Rev. B* **64**, 085318 (2001).
- ¹⁸G. Usaj and H. U. Baranger, *Phys. Rev. B* **63**, 184418 (2001).
- ¹⁹J. Fransson, O. Eriksson, and I. Sandalov, *Phys. Rev. Lett.* **88**, 226601 (2002); **89**, 179903(E) (2002).
- ²⁰Y. Chye, M. E. White, E. Johnston-Halperin, B. D. Gerardot, D. D. Awschalom, and P. M. Petroff, *Phys. Rev. B* **66**, 201301(R) (2002).
- ²¹M. M. Deshmukh and D. C. Ralph, *Phys. Rev. Lett.* **89**, 266803 (2002).
- ²²J. König and J. Martinek, *Phys. Rev. Lett.* **90**, 166602 (2003).
- ²³J. Martinek, Y. Utsumi, H. Imamura, J. Barnas, S. Maekawa, J. König, and G. Schön, *Phys. Rev. Lett.* **91**, 127203 (2003).
- ²⁴J. Martinek, M. Sindel, L. Borda, J. Barnas, J. König, G. Schön, and J. von Delft, *Phys. Rev. Lett.* **91**, 247202 (2003).
- ²⁵M.-S. Choi, D. Sánchez and R. López, *Phys. Rev. Lett.* **92**, 056601 (2004).
- ²⁶N. Sergueev, Q. F. Sun, H. Guo, B. G. Wang, and J. Wang, *Phys. Rev. B* **65**, 165303 (2002).
- ²⁷J. Barnas, R. V. Dugaev, S. Krompiewski, J. Martinek, W. Rudziński, R. Świrkowicz, I. Weymann, and W. Wilczyński, *Phys. Status Solidi B* **236**, 246 (2003).
- ²⁸M. Braun, J. König, and J. Martinek, *Phys. Rev. B* **70**, 195345 (2004).
- ²⁹W. Rudziński, J. Barnas, R. Świrkowicz and M. Wilczyński, *cond-mat/0409386 v2* (2005).
- ³⁰D. L. Klein, R. Roth, A. K. L. Lim, A. P. Alivisatos, and P. L. McEuen, *Nature (London)* **389**, 699 (1997).
- ³¹V. Ranjan, R. K. Pandey, M. K. Harbola, and V. A. Singh, *Phys. Rev. B* **65**, 045311 (2002).
- ³²M. Saitoh and T. Hiramoto, *Jpn. J. Appl. Phys., Part 1* **43**, L210 (2004).
- ³³I. Sandalov, B. Johansson, and O. Eriksson, *Int. J. Quantum Chem.* **94**, 113 (2003).
- ³⁴J. Fransson, *cond-mat/0502289* (2005); *cond-mat/0502290*, *Phys. Rev. B* (accepted).
- ³⁵J. Hubbard, *Proc. R. Soc. London, Ser. A* **276**, 238 (1963).
- ³⁶J. Hubbard, *Proc. R. Soc. London, Ser. A* **277**, 237 (1963).
- ³⁷A. C. Hewson, *Phys. Rev.* **144**, 420 (1966).
- ³⁸C. M. Varma and Y. Yafet, *Phys. Rev. B* **13**, 2950 (1976).
- ³⁹Y. Meir and N. S. Wingreen, *Phys. Rev. Lett.* **68**, 2512 (1992).
- ⁴⁰A.-P. Jauho, N. S. Wingreen, and Y. Meir, *Phys. Rev. B* **50**, 5528 (1994).
- ⁴¹J. Fransson, O. Eriksson, and I. Sandalov, *Phys. Rev. B* **66**, 195319 (2002).
- ⁴²L. P. Kadanoff and G. Baym, *Quantum Statistical Mechanics*, (Benjamin, New York, 1962).
- ⁴³J. Fransson and O. Eriksson, *Phys. Rev. B* **70**, 085301 (2004).
- ⁴⁴J. Fransson, E. Holmström, O. Eriksson, and I. Sandalov, *Phys. Rev. B* **67**, 205310 (2003).
- ⁴⁵A. F. Barabanov, K. A. Kikoin, and L. A. Maksimov, *Solid State Commun.* **15**, 977 (1975).
- ⁴⁶A. F. Barabanov, K. A. Kikoin, and L. A. Maksimov, *Solid State Commun.* **18**, 1527 (1976).
- ⁴⁷Y. A. Izyumov, B. M. Letfulov, and E. V. Shipitsyn, *J. Phys.: Condens. Matter* **6**, 5137 (1994).
- ⁴⁸The condition that $1=N_0+\sum_{\sigma}N_{\sigma}+N_2$ is derived from the property that the total nonequilibrium density of QD states is unity, e.g., $1=\text{Im}\sum_{\sigma}\int\text{tr}\{\mathbf{G}^{<}(\omega)-\mathbf{G}^{>}(\omega)\}d\omega/(2\pi)$.³⁴